NEW ZEALAND SOCIETY FOR EARTHQUAKE ENGINEERING

Shake-table test of flexural RC beams subjected to different levels of repair

K. Miura
Obayashi Corporation, Tokyo, Japan.
The University of Auckland, Auckland, New Zealand.

L.S. Hogan, A.V. Shegay, R. Henry and K. Elwood
The University of Auckland, Auckland, New Zealand.

M. Maeda, T. Nagai, and R. Akiya
Tohoku University, Sendai, Japan.

ABSTRACT

Typically, damaged reinforced concrete (RC) building components are fully repaired to achieve the highest performance recovery. However, this repair objective may not necessarily be essential to achieve building performance that satisfies design criteria and thus be unnecessarily costly and lengthy. In this research, a reasonable strategy of repair termed “partial repair” (in which only the heavily damaged areas of components are repaired) is investigated.

Five identical RC flexural beam specimens were prepared and four of them were subjected to static loading to induce different levels of initial damage (three ‘moderately’ and one ‘heavily’ damaged). One moderately damaged and one heavily damaged specimen were fully repaired while one moderately damaged specimen was partially repaired (i.e., repaired only in the plastic hinge area). The estimated repair cost of partially repaired specimen was 78% of that of the fully repaired specimen. The three repaired specimens, the unrepaired specimen and the undamaged specimen will be subjected to an identical series of gradually scaled dynamic excitations on a shake-table to quantify the differences in performance.

Analytical simulations before the shake-table test were performed. Of the five specimens, the response displacement was the highest for the unrepaired specimen. The responses of the repaired specimens were marginally higher than that of the undamaged specimen; however, the difference between the fully repaired specimen and the partially repaired specimen was insignificant.

1 INTRODUCTION

Typically, damaged reinforced concrete (RC) building components are fully repaired to achieve the highest performance recovery. However, this repair objective may not necessarily be essential to achieve building performance that satisfies design criteria and thus be unnecessarily costly and time-consuming. In this research, a reasonable strategy of repair termed “partial repair” (in which only the heavily damaged areas of components are repaired) is proposed.

Though partially repair can be an optimal repair strategy for some components, structural performance of partially repaired members is unknown while fully repaired members have been tested and the evaluation methods of the performance have been developed (e.g., Marder, 2018, Sarrafzadeh, 2021 and Miura et al., 2023). In addition, in previous studies of fully repaired members, specimens were generally loaded statically and thus the difference of response in earthquakes between undamaged members, fully repaired members and unrepaired members is uncertain.

In this research, a shake-table test of five RC beam specimens (one undamaged specimen, one unrepaired specimen, two fully repaired specimens with different damage levels and one partially repaired specimen) is planned to quantify the difference of responses to given earthquake levels and compare the seismic performance such as stiffness, strength and damping. In this paper, the plan of the test, the test results of the initial loading sequence (static test) to induce damage to the specimens and repair work are introduced. The plan and analytical simulations of the ongoing shake-table test are also presented.

2 EXPERIMENTAL PLAN

2.1 Outline of the test

The outline of the whole test is shown in Figure 1. Five identical RC flexure-governed beam specimens were prepared, four of which were subjected to static loading to induce different levels of initial damage (three ‘moderately’ and one ‘heavily’ damaged). One moderately damaged and the heavily damaged specimen were fully repaired while another moderately damaged specimen was partially repaired (i.e., repaired only in the plastic hinge area). The three repaired specimens, the unrepaired specimen and the undamaged specimen will be subjected to an identical series of gradually scaled dynamic excitations on a shake-table to quantify the differences in performance due to different levels of repair and different damage levels before the repair.

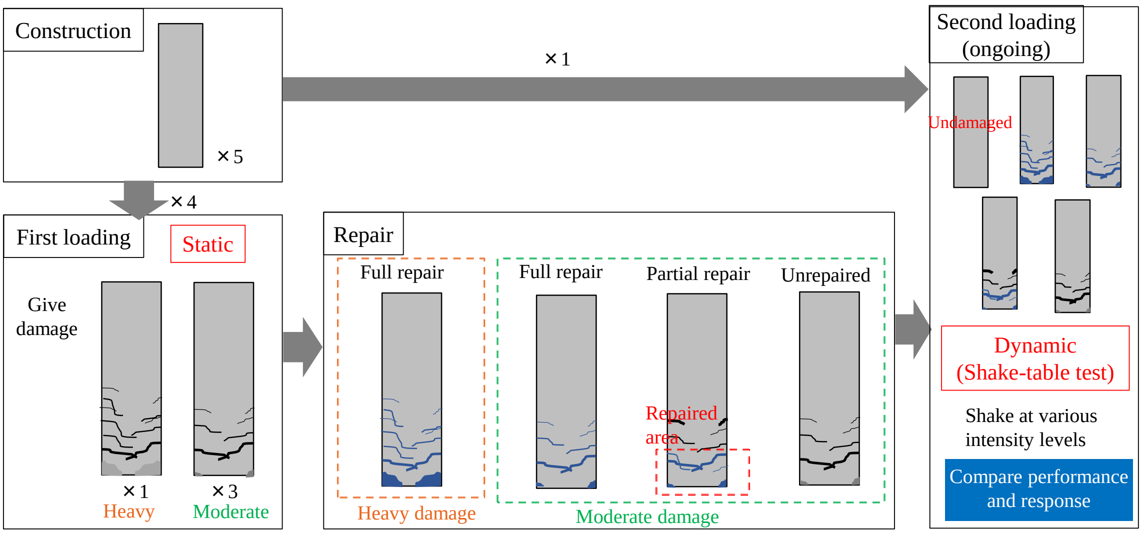

Figure 1: Outline of the test plan.

2.2 Test specimens

The specimens are half-scale cantilever beams. The design originally was adapted from a previous test series by the authors (Miura et al., 2023). The size of the cross section is the same, but the strength of concrete was decreased from the high compressive strength mix of around 50 N/mm^2 used in the previous study to a normal strength mix of around 20 N/mm^2. Additionally, the reinforcement was changed to use New Zealand materials (G500) and the reinforcement ratio adjusted to approximately correspond to that typical in actual buildings by increasing the number of longitudinal bars from three to five. The diameters of reinforcements were the same with those in the previous study (12 mm for longitudinal bars and 6 mm for stirrups) The shear span ratio was also changed to accommodate laboratory requirements.

The list of the specimens is shown in Table 1 and the drawings of the specimens are shown in Figure 2. The letter in the specimen name represent the repair level (UD: undamaged, F: full repair, P: partial repair, UR: unrepaired), while the number indicates the target damage levels after first loading (i.e., loading before repair). Two target damage levels were considered: damage level III and IV. The adopted definitions of damage levels are taken from the JBDPA Guideline (2015), the summary of which is shown in Table 2. Material properties of concrete (test results before first loading) and steel reinforcement are shown Table 3 and Table 4, respectively.

Table 1 List of specimens.

Specimen	Target damage level at first loading	Repair level	Cross-section size (mm)	Reinforcement
UD			200×280	Longitudinal bar: 5-H12 Stirrup: HR6@65 (Discontinuous with 135-degree hooks)
F4	IV	Full		
F3	III	Full		
P3	III	Partial		
UR3	III	Unrepaired		

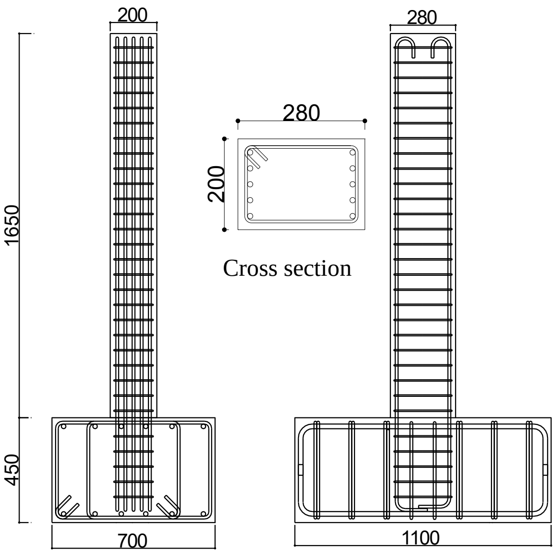

Figure 2: Drawings of specimens.

Table 2: Definition of damage levels of structural members.

Damage level	Observed damage in structural members
I	Sparse cracks can be observed (<0.2 mm). No reinforcement yielding expected.
II	Clearly visible cracks (0.2 - 1 mm) exist. Reinforcement yielding expected.
III	Wide cracks (1 - 2 mm) are present. Plastic hinging mechanisms begin to form. Some spalling of cover concrete is observed but concrete core is in-tact.
IV	Many wide cracks are observed. Compression damage resulting in concrete spalling and exposed reinforcement. Lateral strength degradation may occur, but vertical load is still fully carried by walls and columns.
V	Buckling (and in some cases fracture) of reinforcement, crushing of concrete and vertical deformation of columns and/or shear walls observed. Settlement and inclination of structure are characteristic.

Table 3: Material properties of concrete.

Specimen	Age (day)	Compressive strength (N/mm^2)
UD	75	21.9
F4	38	22.9
F3	54	22.6
P3	63	22.0
UR3	78	18.6

Table 4 Material properties of reinforcement.

Diameter (Grade)	Young's modulus (N/mm^2)	Yield strength (N/mm^2)	Ultimate strength (N/mm^2)
H12(Grade 500)	2.02×10^5	516	697
HR6(Grade 500)	1.79×10^5	500	656

3 FIRST LOADING (STATIC TEST)

3.1 Loading method

The test set up is shown in Figure 3. One horizontal actuator was connected to the upper part of the specimen at 1400 mm above the foundation, and static cyclic loading was performed to damage the specimens to the target damage level shown in Table 1. The loading protocols of each specimen are shown in Figure 4. One initial cycle was applied at 0.125%. Then two cycles were applied at incrementally increasing displacement levels up to 4.0%. For the F4 specimen, one cycle of 5.0% drift was added after 4.0% to induce damage level IV. After the final cycle, the residual displacement was returned to zero.

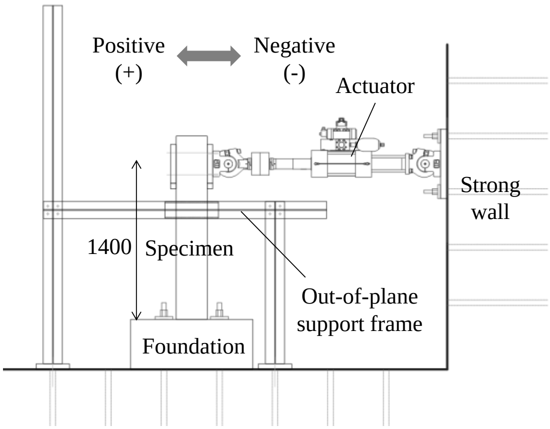

Figure 3: Set up of the static test.

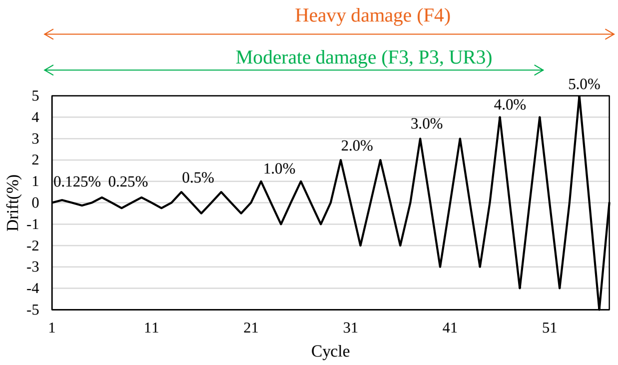

Figure 4: Loading protocols of the static test.

3.2 Test results

3.2.1 Damage process

The damage state of the specimens at 1.0%, 4.0% and 5.0% (only F4) and at the final state after residual displacement was returned to zero is shown in Figure 5. In Figure 5, the maximum residual crack width is also shown. Cracks were observed at 0.125%, and as drift increased, the number of cracks increased and the crack width expanded. Yielding of the longitudinal reinforcement occurred between 1.0% to 1.5% in all specimens. Minor spalling of cover concrete occurred at 3.0% drift and it progressed a little at 4.0% drift. In the F4 specimen, core concrete crushed at negative loading to 5.0% drift and minor buckling of reinforcement was observed.

The damage progression was similar in all specimens, and the final damage state was almost the same in the three specimens intended for moderate damage (F3, P3 and UR3). This was the desired and expected result given the beams had identical designs.

F4	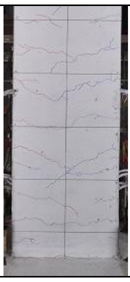				P3	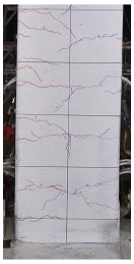		
	1.0% (Crack: 0.15 mm)	4.0% (Crack: 1.9 mm)	5.0% (Crack: 2.0 mm)	Final (Crack: 1.3 mm)		1.0% (Crack: 0.15 mm)	4.0% (Crack: 3.0 mm)	Final (Crack: 2.1 mm)
F3	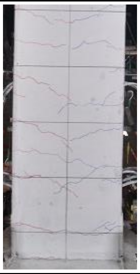				UR3	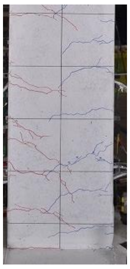	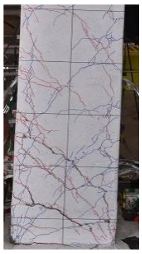	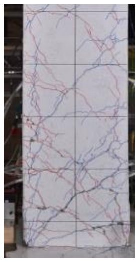
	1.0% (Crack: 0.2 mm)	4.0% (Crack: 3.5 mm)	Final (Crack: 3.0 mm)			1.0% (Crack: 0.08 mm)	4.0% (Crack: 2.5 mm)	Final (Crack: 1.8 mm)

Figure 5: Damage progression seen in the static test.

3.2.2 Load-drift relationships

Shear force – drift relationships for each beam are shown in Figure 6 and the comparison of the backbones is shown in

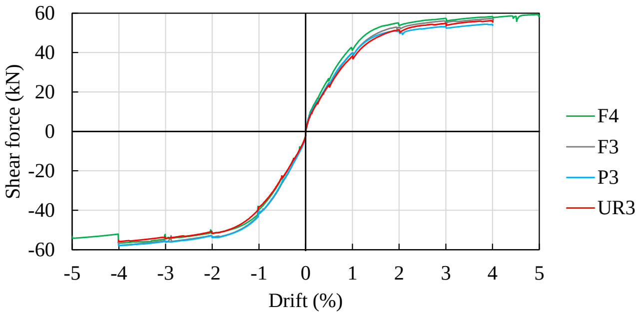

Figure 7. In Figure 6, yielding of longitudinal reinforcement are shown as triangle plot marks. In the moderately damaged specimens (F3, P3 and UR3), no strength deterioration was observed, while in the heavily damaged specimen (F4) the strength deteriorated at -5.0% drift due to the concrete crushing and minor buckling observed. The hysteresis loops and the backbones up to 4% drift are similar in all specimens.

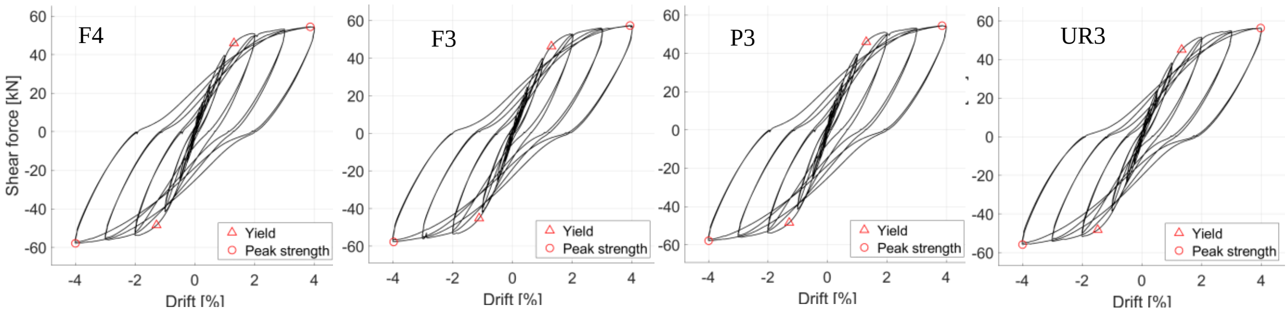

Figure 6: Shear force – drift relationships.

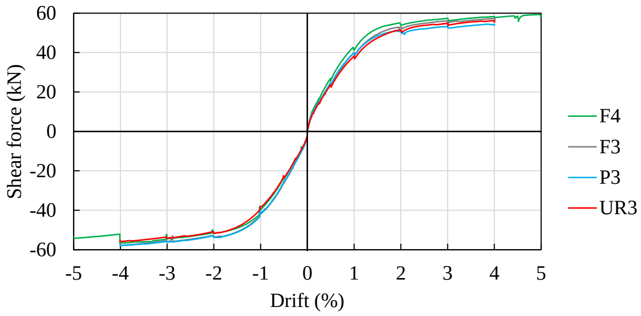

Figure 7: Comparison of backbones for all tested beams.

3.2.3 Investigation on hinge area of the partially repaired specimen

In the partially repaired specimen (P3), only plastic hinge area was planned to be repaired and so the height of the hinge area was investigated based on crack width, curvature distribution and yielding of reinforcement. The damage state and width of major cracks after the static test are shown in Figure 8 while curvature distribution and yielding of longitudinal reinforcement are shown in Figure 10 and **Error! Reference source not found.**, respectively. As shown in Figure 8, some large cracks around 1.2 mm width were observed between 210 mm and 280 mm height above the foundation. Also, Figure 10 shows that curvature was largest under 190 mm height and moderately large between 190 mm and 450 mm height, which indicates that the border of the hinge area is between 190 mm and 450 mm height. In addition, from the data of strain gauges attached to four longitudinal reinforcements at two cross-sections, it was confirmed that all reinforcements yielded at 125 mm height and one of four yielded at the 385 mm height. From these results, the hinge area was assumed to be within the lower 280 mm of the beam, which is equal to the beam depth dimension.

To confirm the validity of the assumed hinge area, crack width distribution in the hinge area and above the hinge area (termed the upper area) was investigated. The cumulative length of each crack width is shown in Figure 11. From this figure it can be seen that most of cracks larger than 0.3 mm are in the hinge area, thus suggesting that the assumed height of 280 mm is reasonable.

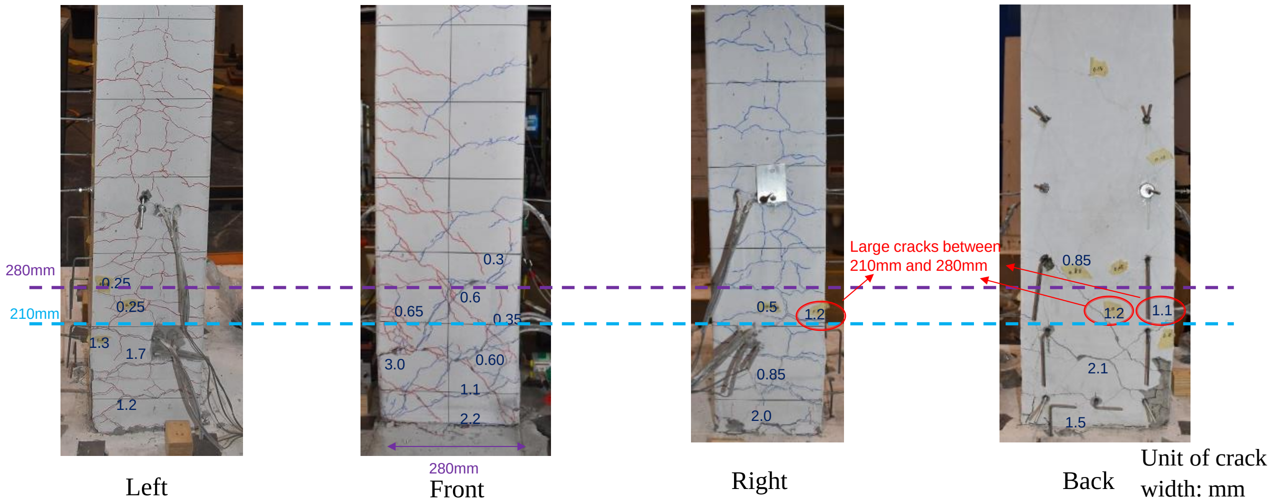

Figure 8: Damage state and crack width of P3 specimen after the static test.

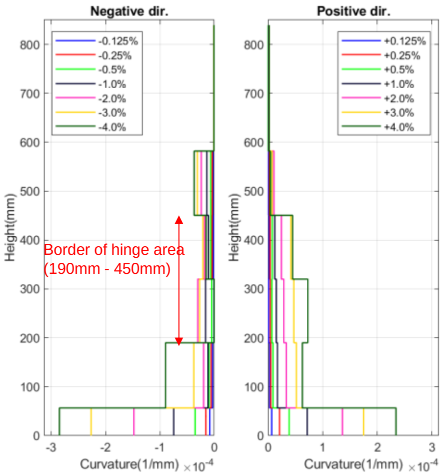

Figure 10: Curvature distribution of P3 specimen.

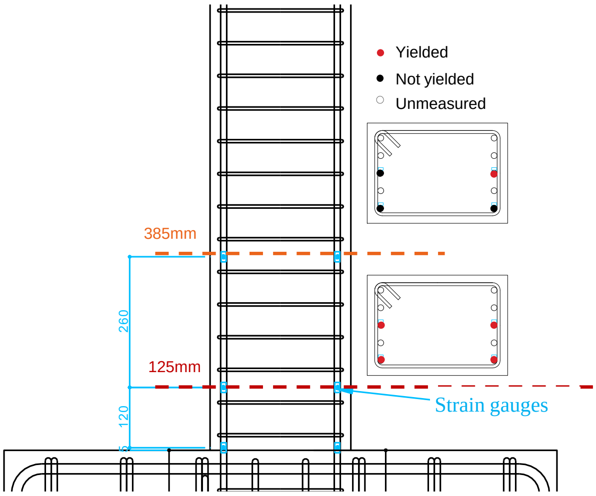

Figure 9 Yielding of longitudinal reinforcements of P3 specimen.

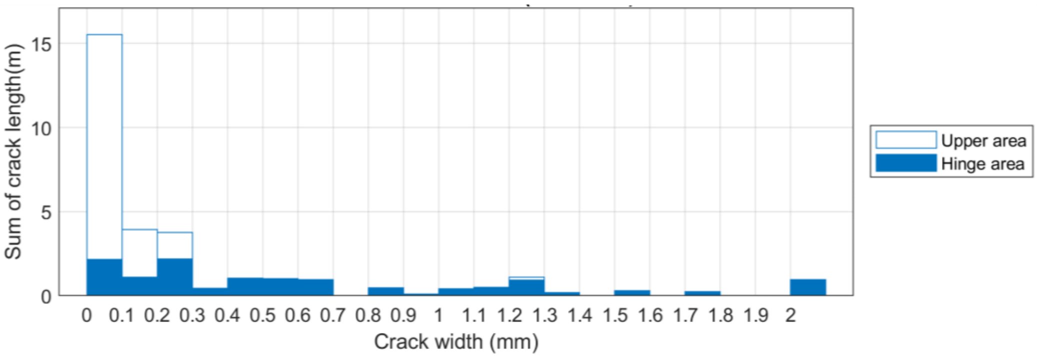

Figure 11: Crack width distribution in the hinge area and the upper area.

4 REPAIR WORK

4.1 Repair strategies

The overall concept of repair work is shown in Table 5. The policy was to use general repair methods practiced in New Zealand. For spalling of concrete, epoxy mortar was used for small areas and grout was applied to severely spalled areas of the F4 specimen. For cracks, an epoxy injection method using an automated pump was adopted. In the fully repaired specimens (F4 and F3), ideally, all cracks should be repaired. However, in this case, only cracks equal to or larger than 0.2 mm width were epoxy injected because injection into cracks less than 0.2 mm was advised by the contractor to be difficult. In the partially repaired specimen (P3), only cracks in the hinge area were repaired. Material properties of the mortar and epoxy from the manufacturer's catalogue are shown in

Table 6, and repair process is shown in Figure 12.

Table 5: Concept of repair work.

Specimen	Damage level	Repair of concrete spalling		Epoxy injection to cracks
		Severe	Minor	
F4	IV (Heavy)	Grout	Epoxy mortar	All cracks (≧0.2 mm)
F3	III (Moderate)		Epoxy mortar	All cracks (≧0.2 mm)
P3	III (Moderate)		Epoxy mortar	Cracks in the hinge area (≧0.2 mm)

Table 6: Material properties of mortar and epoxy.

Material	Product	Tensile strength (N/mm^2)	Compressive strength (N/mm^2)
Epoxy mortar	Sika UA		67 (28 days)
Grout (Castable mortar)	Sika MonoTop 438R		60 (28 days)
Epoxy resin	Sikadur 52	54 (14 days)	57.9 (28 days)

Figure 12 Repair process.

4.2 Repair cost estimation

The repair cost of each specimen was estimated based on the invoice provided by the contractor. As the total cost for the three specimens was shown in the invoice for each work (sealing, injection, grouting etc.), it was distributed to each specimen according to the methods described in Table 7, which were thought to be related to the quantities of work and materials. The estimated repair cost is shown graphically in Figure 13. The repair cost of the P3 specimen was calculated to be 78% of the F3 specimen and this is thought to be due to the reduction of repaired area, given that most of major cracks were repaired. Also, the repair cost of the F4 specimen with heavy damage was just 7% higher than that of the F3 specimen.

Table 7 Cost distribution method to each specimen.

Work	Applied specimen	Cost distribution method
Sealing and cleaning	All	In proportion to sealed area
Epoxy injection	All	In proportion to numbers of injection points
Grouting	F4	All distributed to F4
Administration	All	In proportion to the other cost

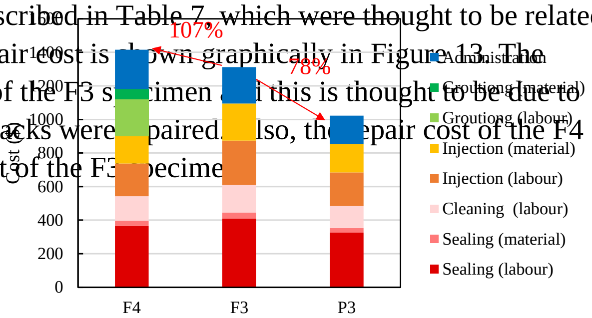

Figure 13 Estimated repair cost.

5 PLAN OF SECOND LOADING (SHAKE-TABLE TEST)

5.1 Shaking method

The test set up is shown in Figure 14. The beam specimen and additional 7 tonne mass are to be installed on the shake-table and connected via a pin-pin strut. Base beams under the mass are fixed on the table and linear bearings are laid between the base beams and the mass to enable the mass to move with the same displacement as the top of the specimen. A safety frame is installed around the mass to avoid excessive displacement.

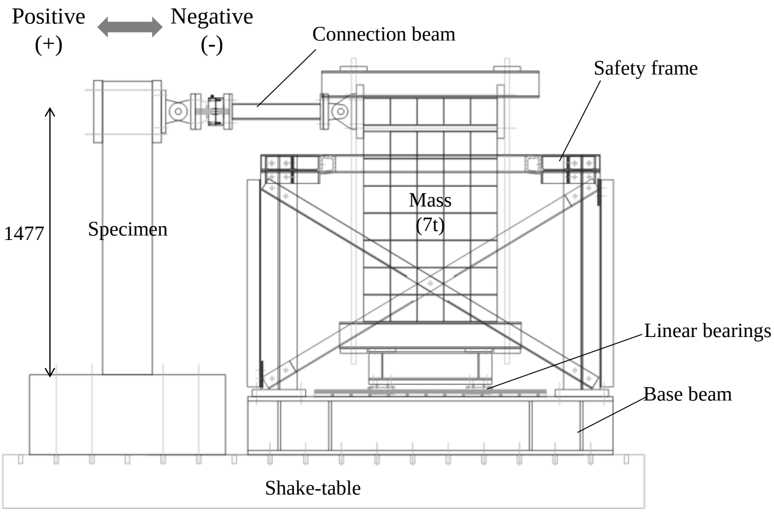

Figure 14: Set up of the shake-table test.

5.2 Shaking protocols

Shakings consist of two phases. The target response of the first phase is service level until yielding and of the second phase is safety level after yielding. As the objective of the first phase is to understand the general tendency of the difference of responses depending on repair levels and damage levels, a seismic motion with minimal site-dependent characteristics (e.g., no peak of response at a certain frequency) is thought to be appropriate. Therefore, an artificial earthquake wave compatible with the Japanese standard response spectrum is used as input. The phases of the artificial motion were based on JMA Kobe record observed in the 1995 Hyogo-ken Nanbu (Kobe) Earthquake. On the other hand, the objective of the second phase is to understand the realistic response for large earthquakes; thus, the observed wave in the 2011 Christchurch Earthquake (NS direction of Station: CCCC) is used. Time histories and acceleration response spectra of the chosen records are shown in Figure 15 and Figure 16, respectively. In the waves, time scale is reduced by 1/√2 of the original records based on the law of similitude considering that the specimens were constructed at a half-scale.

In the shake-table test, the same series of seismic motions shown in Table 8 will be input to the five specimens. The magnifications might be adjusted during the test of the first specimen, but the same protocol will be applied to the following specimens even if it is modified so that the difference in responses to the same input can be obtained.

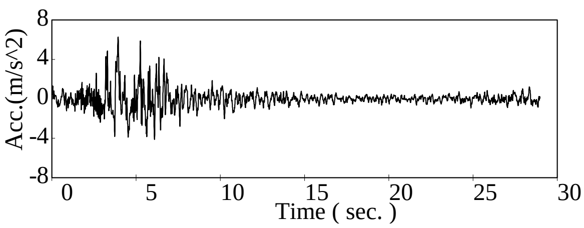

(a) Artificial wave compatible with Japanese design standard

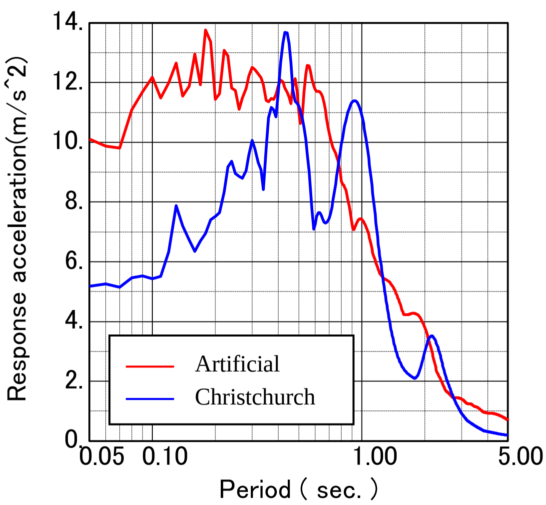

Paper 49 –Shake-table test of flexural RC beams subjected to different levels of repair

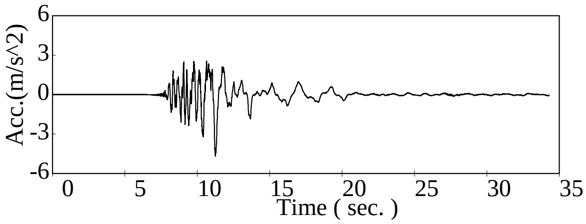

(b) Christchurch wave (Station: CCCC, NS)

Figure 15 Time histories of input waves.

Figure 16 Response spectra of input waves.

Table 8 Shaking protocols.

Phase	Seismic motion	Run	Magnification	Target response
1	Artificial	Run1	5%	Elastic
		Run2	10%	Cracking
		Run3	30%	Before yiedling
		Run4	50%	Yielding
2	Christchurch	Run5	60%	2% drift
		Run6	70%	3% drift
		Run7	90%	4% drift
		Run8	120%	5% drift

6 ANALYTICAL SIMULATION BEFORE SHAKE-TABLE TEST

Analytical simulations before the shake-table test were performed to estimate the response in the test.

6.1 Analytical models

The beam specimens were idealized as non-linear single-degree-of-freedom models with equivalent shear and rotational springs. The steps for developing backbones of the models are shown in Figure 17 and are described below.

(1) Repaired specimens (F4, F3 and P3)

1. The force – drift relationship in the static test was reduced to a tri-linear backbone using the method shown in Miura et al. (2023).
2. The initial stiffness and the yielding stiffness of the tri-linear backbones were reduced by multiplying by recovery factors φ_{si} and φ_{sy}, respectively. The values for these recovery factors for the fully repair specimens (F4 and F3) were adopted previous research by the authors (Miura et al., 2023). As there is no reference regarding recovery factors of partially repaired components, the values were set a little smaller than those of the fully repaired specimens as shown in Figure 17.
3. The stiffness after yielding was assumed as 1/1000 of the initial stiffness.

(2) Undamaged specimens (UD)

The tri-linear backbone of F4 was used (as this specimen had the closest concrete strength to specimen UD).

(3) Unrepaired specimen

A bi-linear model with stiffness equal to the secant stiffness at the final drift (4%) of the static test was used. As the backbone from the static test had a positive and a negative direction, the average value of the stiffness in both directions was used. Backbones constructed by the methods described above are shown in Figure 18.

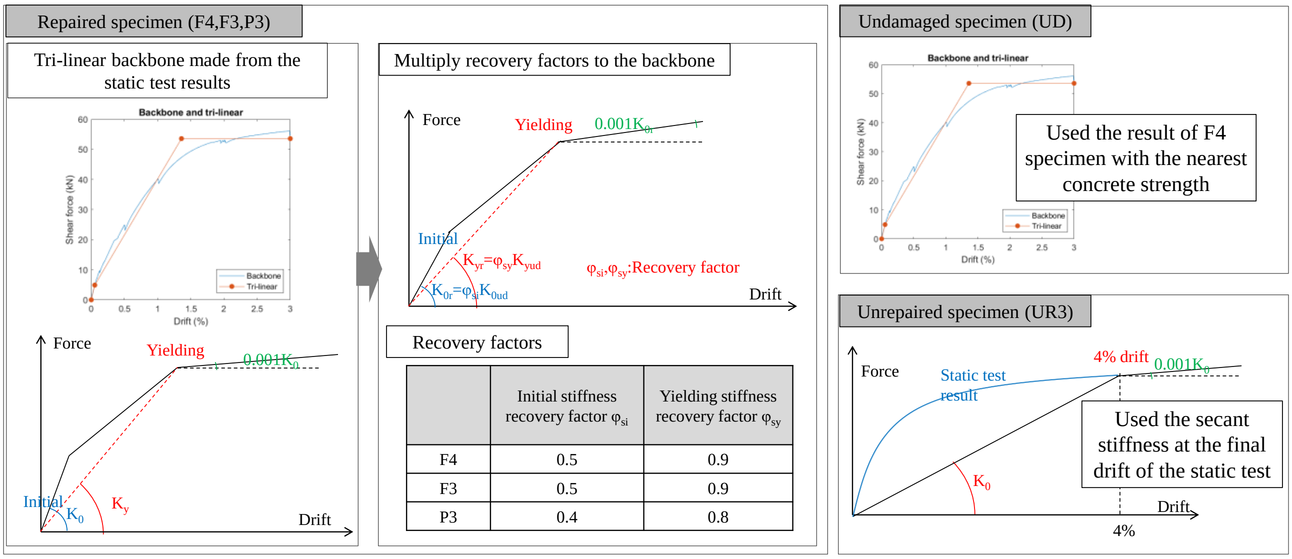

Figure 17 How to make backbones of analytical models.

As a hysteresis model, Takeda model was used for UD and UR3 specimens and Takeda-slip model was used for the repaired specimens (F4, F3 and P3). In the repaired specimens, damping recovery factors φ_h were used to consider the deterioration of hysteretic damping. As shown in Figure 19, slip factors were set so that the hysteresis areas are φ_h times that of the undamaged component (Takeda model) at 3% drift. The values of recovery factors φ_h were taken from the database developed by Mikawa et al., (2022).

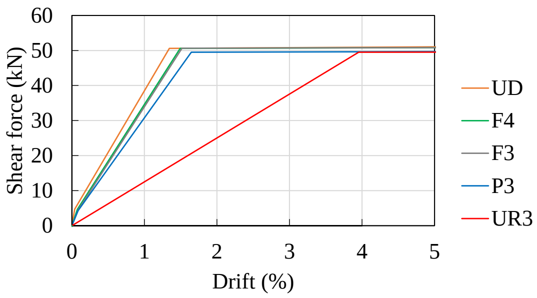

Figure 18 Backbones of analytical models.

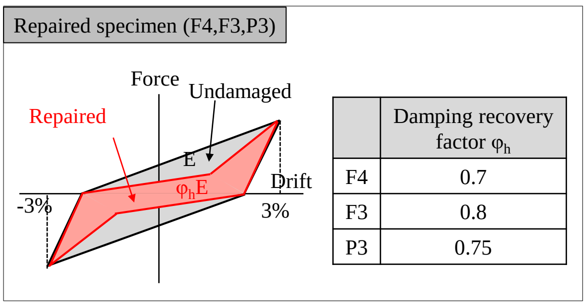

Figure 19 Hysteresis models of the repaired specimens.

6.2 Input waves for simulations

A series of seismic motions consistent with the shaking protocols shown in Table 8 was inputted. The time history of the motions is shown in Figure 20

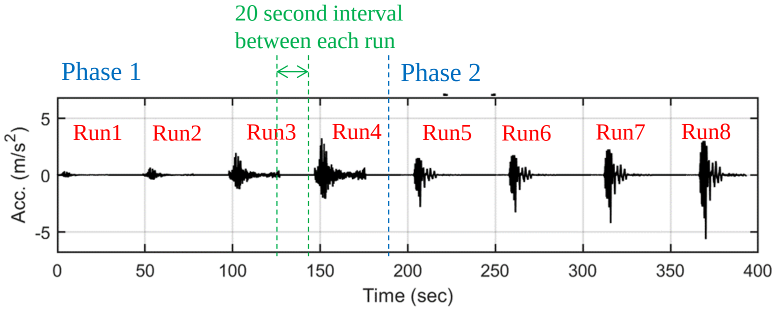

Figure 20 Input waves for analytical simulations.

6.3 Analytical results

(1) Phase 1 (before yielding)

The analytical responses for phase 1 are shown in Figure 21. In Figure 21(d)(e), the ratios of responses to the undamaged specimen (UD) are shown. As shown in Figure 21(a), the four specimens except UR3 reached near yielding drift as planned. Regarding the response drifts, they were much higher (8 to 9 times at Run 1 and 2 and 3 to times at Run 3 and 4) in the unrepaired specimen (UR3). Figure 21(b)(d) show that the response drifts in the repaired specimens were a little larger (2 to 2.5 times at Run 1 and 2 and 1.2 to 1.5 times at Run 3 and 4) than those of the undamaged specimen (UD). However, there is little difference between the partial repair (P3) and the full repair (F3 and F4). The difference by damage levels (between F3 and F4) was insignificant. The acceleration responses were quite similar in all the specimens as shown in Figure 21(c)(e).

(2) Phase 2 (after yielding)

The analytical responses for phase 2 are shown in Figure 22. In Figure 22(c)(d), the ratios of responses to the undamaged specimen (UD) are also shown. Regarding the response drifts, the difference between the unrepaired specimen (UR3) and the other specimens was smaller than phase 1, but UR3 still had higher responses (around twice of those of UD until Run 6 and 1.2 to 1.6 times at Run 7 and 8). Figure 22 (a)(c) show that the response drifts in the repaired specimens were a little larger (1.2 to 1.6 times) than the unrepaired specimen until Run 6 (around 3% drift). However, they became almost the same after Run 7. Also, there is little difference between the partial repair (P3) and the full repair (F3 and F4) overall. The difference by damage levels (between F3 and F4) was insignificant in all cases. The acceleration responses were almost the same except the Run 5 of the unrepaired specimen in which the response did not reach yielding strength. Common to both phases, the responses of the partially repaired specimen were not much different from those in the fully repaired specimens. Therefore, the partial repair appears to be a reasonable strategy for cost-efficient repairs. However, verification still needs to be conducted via shake-table tests.

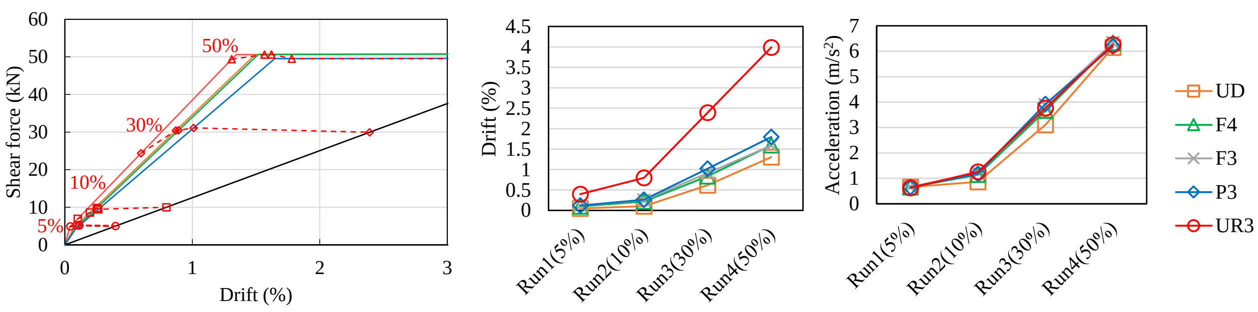

(a) Responses on the backbones (b) Response drift (c) Response acceleration

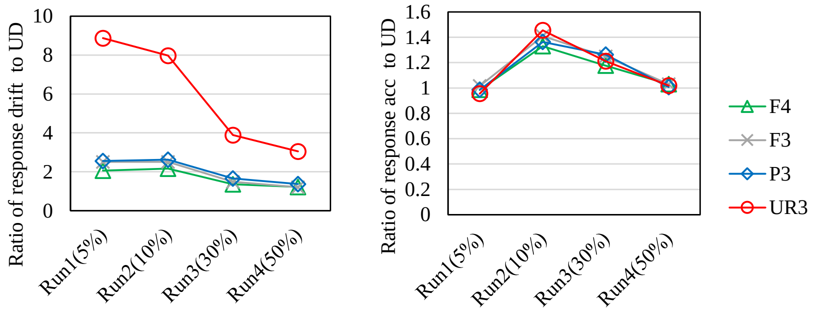

(d) Ratio of response drift to UD (e) Ratio of response acceleration to UD

Figure 21 Analytical results for phase 1 (before yielding)

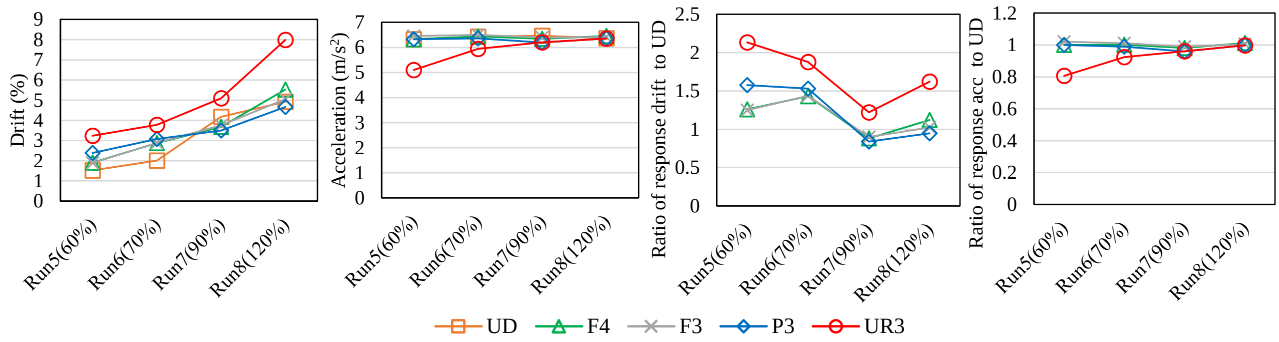

(a) Response drift (b) Response acceleration (c) Ratio of response drift to UD (d) Ratio of response acceleration to UD

Figure 22 Analytical results for phase 2 (after yielding)

7 CONCLUSIONS

- To investigate optimal repair strategies in terms of cost effectiveness, a shake-table test of RC beams subjected to different levels of repair and different damage levels was planned. Five identical RC flexural beam specimens were prepared and four of them were subjected to static loading to induce different levels of initial damage (three 'moderately' and one 'heavily' damaged). The three repaired specimens, the unrepaired specimen and the undamaged specimen will be subjected to an identical series of gradually scaled dynamic excitations on a shake-table to quantify the differences in performance. The following findings have been obtained from the preliminary study:
- One moderately damaged and one heavily damaged specimen were fully repaired while one moderately damaged specimen was partially repaired. The repair cost of partially repaired specimen was 78% of that of fully repaired specimen.
- Analytical simulations before the shake-table test were performed. Of the five specimens, the response displacement was the highest for the unrepaired specimen. The responses of the repaired specimens were marginally higher than that of the undamaged specimen; however, the difference between the fully repaired specimen and the partially repaired specimen was insignificant.

The above results suggest a cost-saving can be obtained from partial repair approaches without a significant detriment to the performance. Shake-table testing is underway to prove this experimentally.

8 ACKNOWLEDGEMENT

This research was funded by JSPS KAKENHI Grant-in-Aid for Fostering Joint International Research (B), Grant Number JP21KK0074. Also, part of the shake-table test was funded by QuakeCoRE DT2 "Whole-of-Building Seismic Performance". The authors would like to express their gratitude for the support.

9 REFERENCES

Japan Building Disaster Prevention Association (JBDPA). (2015), *"Guidelines for Post-earthquake Damage Evaluation and Rehabilitation of RC Buildings"*. Japan Building Disaster Prevention Association., Tokyo, Japan.

Marder K.J. (2018). *"Post-Earthquake Residual Capacity of Reinforced Concrete Plastic Hinge"*. Ph.D. Dissertation, Department of Civil and Environmental Engineering, University of Auckland, Auckland, New Zealand, 302pp.

Mikawa A., Akiya R, Nagai T, Shegay A, Miura K, Maeda M, and Seki M (2022). "Evaluation for recovery of stiffness, strength and hysteresis damping by repair based on database of structural tests of damaged RC members", *Japan Association for Earthquake Engineering (JAEE) Annual Meeting, 15-16 December, Sapporo, Japan,* Paper No.Ts_20220096.

Miura K., Anabuki T, Yonezawa K, Mikawa A, Nagai Tomoki, Maeda M, Shegay A. and Seki M (2023). "Experimental study on structural performance and damage characteristics of repaired flexural RC members", *New Zealand Society for Earthquake Engineering (NZSEE) Annual Technical Conference, 19-21 April, Auckland, New Zealand,* Paper No.113.

Sarrafzadeh M.M. (2021). *"Residual Capacity and Reparability of Moderately Damaged Reinforced Concrete Ductile Frame Structures"*. Ph.D. Dissertation, Department of Civil and Environmental Engineering, University of Auckland, Auckland, New Zealand, 463pp.